ACS OMEGA

http://pubs.acs.org/journal/acsodf

Article

Wettability and Its Influencing Factors of Tight Sandstones in Coal Measures in Ordos Basin, China

Xuejuan Song, Yong Qin, and Hao Ma*

Cite This: *ACS Omega* 2022, 7, 28503−28515

Read Online

ACCESS | Metrics & More | Article Recommendations

ABSTRACT: With the recent development in exploration technology, extensive attention has been given to the tight sandstone gas reservoirs in coal measures. As a surface property of tight sandstone, wettability is a very important factor that controls the distribution and transport of gas and water inside the sandstone; thus, it plays a vital role in the sandstone gas-recovery process. In this study, a series of tests, namely, the Amott−Harvey wettability test, contact angle test, ζ-potential test, X-ray diffraction, thin-section analysis, scanning electron microscopy, and mercury intrusion porosimetry, were conducted to investigate the basic features of tight sandstones in coal measures and the effects of petrological characteristics, fluid properties, the underground environment, sedimentation, and diagenesis on the wetting behavior of sandstone. The impacts of three major forces, namely, the structural, electrostatic, and dispersion forces, on sandstone wettability were also discussed. The results showed that high surface roughness, high textural and compositional maturity, low organic matter content, a strong hydrodynamic sedimentary environment, weak compaction and cementation, high temperature, and high solution pH, as well as a low ionic concentration, enhance the hydrophilicity of the sandstone.

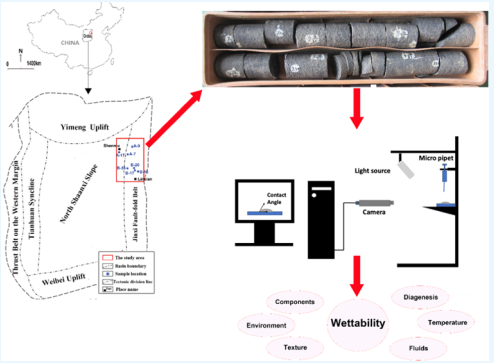

1. INTRODUCTION

As a fundamental physical property, wettability is a major factor controlling the distribution, flow, and location of fluids (gas, crude oil or brine) in reservoir rock. Usually, hydrophilic reservoir rock means that the wetting fluid can be imbibed spontaneously into the rock by displacing the nonwetting fluid. Wettability could significantly affect the oil or gas recovery from sandstone reservoirs.[1,2]

Wettability is generally considered to be determined by the interface interactions between the sedimentary rocks and the fluids existing within the pores; thus, rock surface and fluid properties are mainly discussed and explored in this work. Regarding rock surface properties, it was reported that the surface chemical composition (surface contamination, mineral composition, and content) and microgeometric structure (pore size distribution, porosity, permeability, and surface roughness), as well as the static and dynamic interface properties, greatly contribute to sandstone wettability.[3] Regarding fluid properties, wetting-alternation mechanisms, including pH change, acid/base interactions, ion binding, and polar interactions, reportedly affect surface charge at liquid−liquid or solid−liquid interfaces.[4−11] Changes in the geological environment of these reservoir rocks, such as the sedimentary environment, may also be an influencing factor in sandstone wettability and will be discussed in this work.

Although a considerable amount of attention has been focused on wettability research, understanding the wettability of rock is still a very challenging problem because the surfaces of sandstone rocks are complicated mixtures of minerals, where the rock properties are determined by a delicate interplay of many different effects.[12] In our project, we directly performed tests using tight sandstone samples obtained from coal measures rather than just using one or several minerals to investigate the wettability of sandstone.[13−18]

The coal measures in Ordos Basin have the following characteristics: Sandstones have a large cumulative thickness but small monolayer thickness. In addition, there are many types of source rocks with fairly high organic content that produce a significant amount of hydrocarbon gas. Included in this group are a vertically cyclic combination of coal seams, mudstones or shales, and sandstones as well as coexisting coal, coalbed gas, shale gas, and tight sandstone gas.[19] All of these characteristics make sandstones a good source for gas exploration and development. With the recent development in gas exploration technology, tight gas has already been used as an important replacement for conventional natural gas.[20−23] The sandstone

Received: May 26, 2022
Accepted: July 15, 2022
Published: August 2, 2022

https://doi.org/10.1021/acsomega.2c03288
ACS Omega 2022, 7, 28503−28515

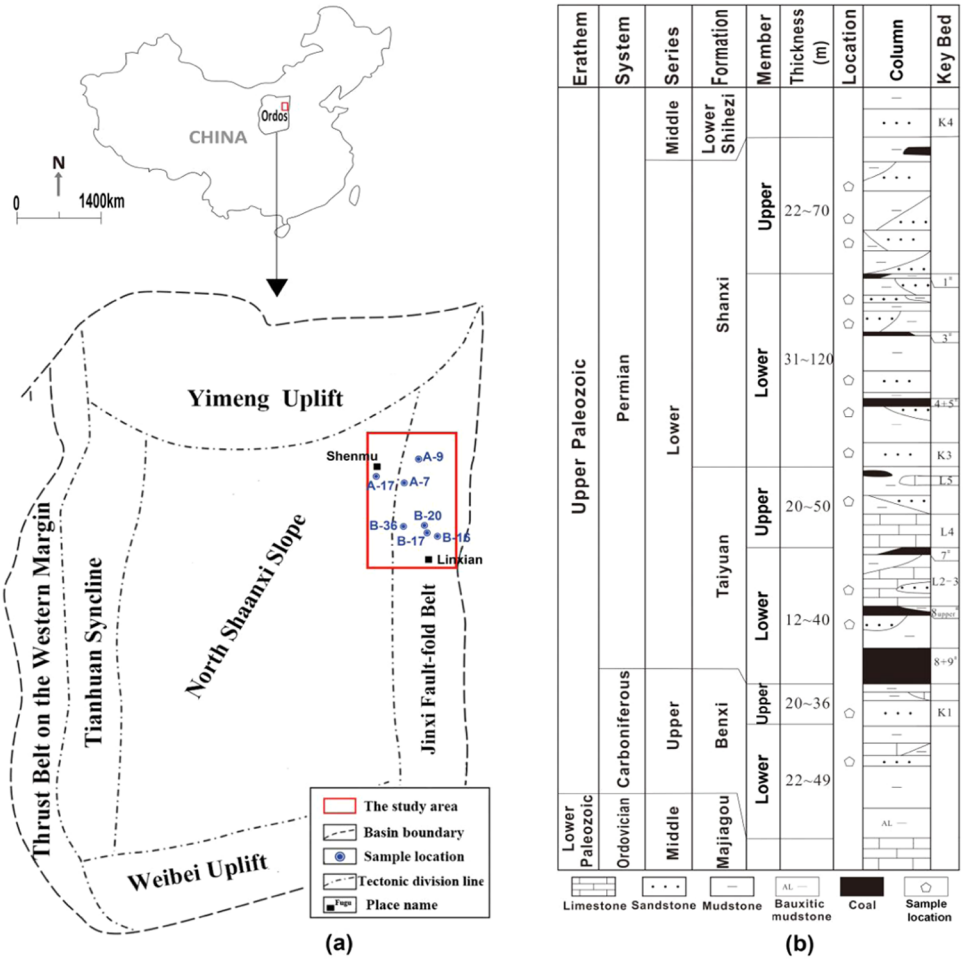

Figure 1. Sandstone sampling information.

wettability studies in the Ordos area mostly focus on the oil reservoir of the Upper Triassic Yanchang Formation. Scholars found that oil-bearing sandstones in Yanchang Formation were mixed wet, and it can be explained that there are a lot of chlorites in the sandstone, which adsorbed polar compounds and mostly became oil-wet. There are few studies on the wettability of carboniferous-Permian tight gas reservoir sandstones.[21,22] Considering that the wettability and its influencing factors play a vital role during the process of water flooding in the development of gas reservoirs, we carry out this research for providing guidance for subsequent industrial applications.

2. MATERIALS AND EXPERIMENTAL METHODS

2.1. Sandstone Sampling Information. As shown in Figure 1a, 29 tight sandstone samples were collected from the Linxing-Shenfu area located in the northeast section of Ordos Basin, China. The samples are distributed within the Benxi, Taiyuan, and Shanxi Formations of Upper Paleozoic with depths of 1700−2100 m, as shown in Figure 1b.

2.2. Experimental Methods. *2.2.1. Petrology and Pore Structure Characterization.* For sandstone petrology and pore structure characterization, X-ray diffraction (XRD, D/max-2600 X-ray diffractometer, Rigaku) tests were performed to obtain the sandstone mineral composition and content, thin-section analysis (DM4500P optical microscope, Leica) and scanning electron microscopy (SEM, Quanta 450FEG, FEI) were used to characterize the sandstone microstructure and morphology, and mercury intrusion porosimetry (MIP, AutoPore IV Mercury Porosimeter) tests were performed to obtain its porosity and permeability. These tests were carried out in the experimental center of CNOOC (China National Offshore Oil Corporation).

2.2.2. Sandstone Wettability Measurement. Sandstone wettability measurements were obtained through the Amott−Harvey test and contact angle measurement. These two methods are generally used to fully determine the rock wetting behavior toward water or oil. They are discussed as follows:

2.2.2.1. Standard Amott−Harvey Test. The Amott−Harvey method is a widely accepted testing technique to measure the wettability of sandstone rocks. These tests were also performed in the experimental center of CNOOC. The water used was a 30 g/L $CaCl_2$ solution, mimicking the isomineralization underground water, while the oil was a synthetic oil with a density of 0.7755 g/cm^3 and a viscosity of 1.0562 mPa/s^{-1} at 25 °C. Four displacement tests were conducted at 30 °C, and the wettability index (I) can be calculated as follows[2]

$$I = W_w - W_o = \frac{V_{o1}}{V_{o1} + V_{o2}} - \frac{V_{w1}}{V_{w1} + V_{w2}} \quad (1)$$

where W_w, W_o, V_{o1}, V_{o2}, V_{w1}, and V_{w2} represent the water index, oil index, the volume of oil for spontaneous displacement of water (mL), the volume of oil for the forced displacement of water (mL), the volume of water for the spontaneous displacement of oil (mL), and the volume of water for the forced displacement of oil (mL), respectively.

https://doi.org/10.1021/acsomega.2c03288
ACS Omega 2022, 7, 28503−28515

The wettability index (I) can be used to reflect the water-wetting behavior of sandstone. A sandstone is considered as strongly water-wet when I is between 0.7 and 1.0, while it is considered to be moderately water-wet when $0.3 < I \leq 0.7$ and weakly water-wet when $0.1 < I \leq 0.3$.[2]

2.2.2.2. Contact Angle Measurement. This method was used to reflect the change in the sandstone hydrophilicity with different surface roughness. These tests were carried out in the laboratory of material engineering, China University of Mining and Technology. Sandstone was cut into three small samples with a thickness of 1 cm and a diameter of 2.5 cm. Then, the surfaces of the samples were initially polished with coarse sandpaper, and each sample was finished with #600, #1500, and #2000 sandpaper (Matador, Germany), respectively. An FTA-200 dynamic contact angle analyzer was utilized to measure the contact angle between the sandstone sample and the water droplet. Five tests were performed on each sample surface and an average value was obtained. The schematic of the experimental setup is shown in Figure 2.

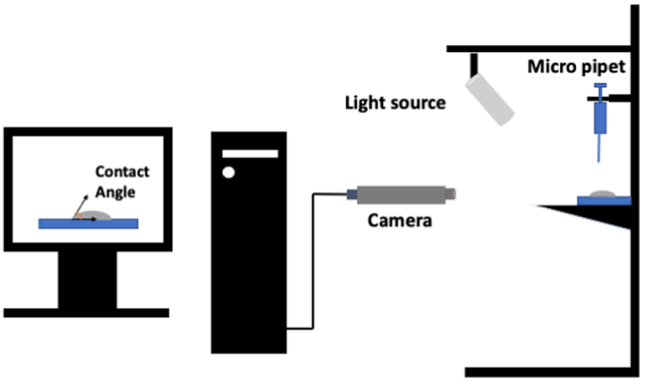

Figure 2. Schematic of the experimental setup used for contact angle measurement.

2.2.3. Experiment on the Influence of Fluid and Temperature. The fluid present in the sandstone pores significantly affects the rock wetting behavior. To find out how it works, a series of Amott−Harvey tests and contact angle measurements were conducted varying the liquid type, salinity, pH, and temperature to explore the impacts of these factors on the wettability of tight sandstone and they are discussed as follows.

2.2.3.1. Liquid Temperature. The Amott−Harvey tests were performed on six representative samples by adjusting the water bath temperatures to 30, 40, and 60 °C while keeping other testing parameters constant.

2.2.3.2. Liquid Type, Salinity, and pH. The Amott−Harvey tests and contact angle measurements were performed on these six sandstone samples by varying the liquid type ($CaCl_2$, $NaHCO_3$), salinity ($CaCl_2$ concentration of 0, 3, and 30 g/L), and pH (5, 7, 8.5).

2.2.3.3. ζ-Potential Measurements. A NanoBrook ZetaPlus analyzer (Brookhaven) was used to obtain the electrostatic repulsion forces of sandstone particles under different pH values. The sandstone samples were ground into very fine particles and then suspended in 200 mL of a NaCl solution at a concentration of 10^{-3} mol/L. The pH range investigated was from 3 to 10 with a step increase of 1 unit and an equilibration time of 5 min for each measurement. These measurements were performed in the laboratory of mining and materials engineering, McGill University.

3. RESULTS AND DISCUSSIONS

3.1. Standard Amott−Harvey Test Results. The wettability of 29 sandstone samples through the Amott−Harvey method is listed in Table 1. As shown in Table 1, the wettability indexes of these samples range from 0.21 to 0.79. These sandstone samples generally have high water-wet indices (average 0.81) and low oil-wet indices (average 0.29), which indicates that the affinity of sandstones to water is stronger than that to oil. Based on the criteria in Section 2.2.2.2, they are all considered to be water-wet, which is in agreement with previous studies.[19] Overall, 38% of the sandstones are strongly water-wet, 24% are moderately water-wet, and 38% are weakly water-wet.

Table 1. Sandstone Wettability through the Standard Amott−Harvey Method

sample no.	water index (r_w)	oil index (r_o)	wettability index $I = r_w - r_o$	wettability
1	0.90	0.27	0.63	moderately water wet
2	0.77	0.50	0.27	weakly water wet
3	0.88	0.19	0.69	moderately water wet
4	0.92	0.20	0.72	strongly water wet
5	0.86	0.14	0.71	strongly water wet
6	0.83	0.23	0.60	moderately water wet
7	0.90	0.18	0.72	strongly water wet
8	0.70	0.45	0.25	weakly water wet
9	0.94	0.31	0.63	moderately water wet
10	0.83	0.08	0.75	strongly water wet
11	0.75	0.45	0.30	weakly water wet
12	0.88	0.19	0.69	moderately water wet
13	0.89	0.20	0.69	moderately water wet
14	0.64	0.40	0.24	weakly water wet
15	0.67	0.38	0.29	weakly water wet
16	0.89	0.14	0.75	strongly water wet
17	0.71	0.43	0.28	weakly water wet
18	0.73	0.42	0.31	moderately water wet
19	0.94	0.23	0.71	strongly water wet
20	0.83	0.11	0.72	strongly water wet
21	0.73	0.45	0.27	weakly water wet
22	0.86	0.14	0.71	strongly water wet
23	0.67	0.40	0.27	weakly water wet
24	0.91	0.12	0.79	strongly water wet
25	0.83	0.10	0.73	strongly water wet
26	0.88	0.17	0.72	strongly water wet
27	0.67	0.40	0.27	weakly water wet
28	0.71	0.50	0.21	weakly water wet
29	0.75	0.50	0.25	weakly water wet

The reason why all of these sandstones are water-wet can be attributed to the kerogen type of the source rock in the coal

https://doi.org/10.1021/acsomega.2c03288
ACS Omega 2022, 7, 28503−28515

measures where the sandstones are located. Initially, all sandstones were water-wet prior to the injection of oil and gas because they were deposited in rivers, lakes, or marine-continental transitional environments.[2] For tight sandstone in oil reservoirs, the source rock is the mudstone or shale, which was formed in a deep-water environment (ocean or deep lake) and is rich in type I and type II kerogen. For tight sandstones in coal measures, the source rock is the coal, mudstone, or shale, which is deposited in the environment far away from deep water and is rich in type III kerogen. After being heated by geothermal energy, a significant amount of oil and gas was produced from type I and type II kerogen, while only gas was produced from type III kerogen. In the first case, the migration and accumulation of oil would drive its polar end to absorb on the sandstone pore surface, followed by the exposure of the hydrocarbon end, resulting in the transformation of sandstone to oil-wet.[24,25] In the second case (our case), the gas would be transported into the sandstone to drive away most of the original pore water. However, some water would be retained by capillary forces in the finer pore spaces or as films on pore surfaces, keeping the sandstone water-wet.[24]

3.2. Contact Angle Test Results. When the samples were cut from sandstones with a diamond saw, the surfaces needed to be polished flat prior to the contact angle tests. The higher the sandpaper model number, the smoother the polished sandstone surface, and thus the lower the surface roughness. The results of contact angle tests are listed in Table 2.

Table 2. Results of Contact Angle Tests

	sandpaper model number		
sample no.	#600	#1000	#2000
1	18.19	19.24	22.61
2	27.04	28.56	38.88
3	18.94	25.94	28.60
4	24.49	25.19	27.28
5	25.68	27.91	28.53
6	32.75	33.00	33.69
7	17.81	18.72	19.25
8	20.87	23.06	29.33
9	17.68	18.47	27.81
10	27.39	27.55	28.05
11	22.54	38.40	41.03
12	19.41	27.35	27.99
13	14.56	15.54	27.52
14	24.32	26.37	33.59
15	42.09	42.22	43.86
16	23.38	23.54	23.87
17	32.33	36.61	37.26
18	35.11	35.98	42.68
19	21.37	21.83	22.74
20	13.00	13.17	17.50
21	23.63	25.15	29.90
22	17.87	22.44	26.06
23	57.66	77.15	83.77
24	14.44	15.76	17.20
25	16.69	19.94	23.40
26	18.49	21.20	21.68
27	27.38	28.17	30.51
28	27.95	28.92	34.65
29	35.81	42.68	49.45

The results show that the contact angles of all of the sandstone samples are less than 90°, further indicating that they are all water-wet. The two tables above yield this conclusion: in general, with the increase in the wettability index, the contact angle is decreased. When the wettability indices are between 0.1 and 0.3 (weakly water-wet), 0.3 and 0.7 (moderately water-wet), and 0.7 and 1.0 (strongly water-wet), the corresponding contact angles are approximately between 80 and 40, 40 and 25, and 25−10°, respectively. With the increase in the surface roughness of sandstones (decrease in the sandpaper model number), the contact angles between water and the sandstone surface decrease, indicating that the hydrophilicity of the sandstone increases. This can be explained as follows: as the roughness of the sandstone surface increases, its surface becomes more undulating, and a larger number of polar chemical bonds are exposed on the surface of the sandstone per unit area, which increases the sandstone surface energy and enhances water molecule attraction. Thus, the sandstone surface shows stronger hydrophilicity.[26,27]

3.3. Impacts of Sandstone Properties on Wettability.

3.3.1. Impacts of Mineral Components and Contents. Through XRD analysis, the minerals in the sandstone are: quartz, illite, kaolinite, chlorite, K-feldspar, albite, pyrite, calcite, siderite, and ankerite. The quartz range is 46.2−87.1% with an average value of 66.7%. The clay mineral contents are as follows: illite content 0.8−29.8% with an average value of 14%, kaolinite content 0.3−21.5% with an average value of 5.5%, and chlorite 0.1−15.1% with an average value of 1.1%. The feldspar content is 1.6−15.1%, with an average value of 3.7%.

It is generally considered that the sandstone wettability is determined by surface forces in the thin films between solid−liquid surfaces, in which structural, dispersion, and electrostatic forces are the three main components.[28,29] The surface composition of sandstone mainly affects the magnitude of structural forces; they are the short-range forces between hydrophilic surfaces in water, and these forces arise from the energy needed to dehydrate interacting surfaces, which contain polar species.[30−32] A larger number of these bonds with a higher polarity result in a higher sandstone surface energy when the sandstone surface interacts with water films, resulting in higher sandstone hydrophilicity.

Among these minerals, quartz, illite, and kaolinite show very strong water-wetting behavior. This can be explained as follows:

Quartz (SiO_2) has a diamond structure with one silicon atom covalently bonded with four oxygen atoms. The following reactions may occur when the fractured surface composed of the highly reactive undercoordinated silicon and oxygen bonds makes contact with water films[33]

https://doi.org/10.1021/acsomega.2c03288
ACS Omega 2022, 7, 28503−28515

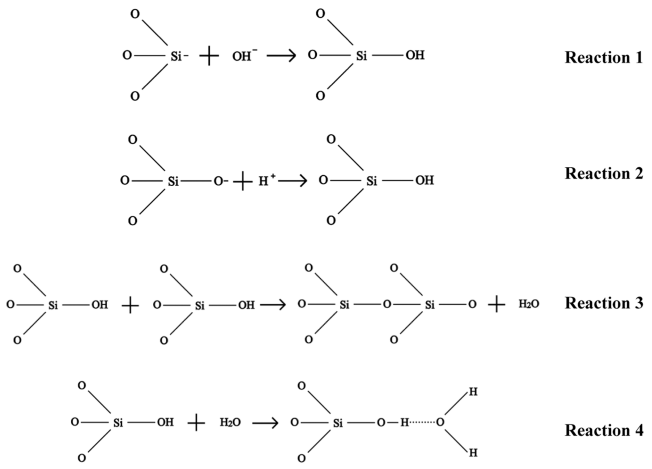

Mineral wettability depends on the surface energy of the mineral. A strong polarity of the covalent bond or ionic bond broken on the mineral surface or a high number of broken bonds and the unsaturated bond strength will bring a high mineral surface energy. When encountering with water, the polar bonds on the surface of the mineral form chemical bonds with H^+ and OH^- in the water and further form hydrogen bonds with water molecules. The stronger the structural force, the higher the hydrophilicity of the mineral surface. As shown in Reactions 2−5, the interior of quartz (SiO_2) has a silicon−oxygen tetrahedron structure, and the Si−O bond is broken on the surface. These residual bonds have high polarity and can interact with water molecules to produce silanol groups (Si−OH). The adjacent silanol groups can be further dehydrated to form siloxane bonds (Si−O−Si); alkane alcohol groups can also form hydrogen bonds with water molecules. It is the structural force between the broken bond on the quartz surface and the water that makes quartz highly hydrophilic.

For kaolinite ($Al_4[Si_4O_{10}](OH)_8$), the polar bond energy on the surface caused by the hydrogen bonds and the broken Si−O and Al−O bonds is very high, which causes the high hydrophilicity of this mineral.[34] For illite ($K_{1-x}(H_2O)_x\{Al_2[AlSi_3O_{10}](OH)_{2-x}(H_2O)_x\}$), the appearance of the hydrogen bond, K^+ ionic bond, and a larger number of broken Si−O and Al−O bonds on its fractured surface causes higher bond energy and hydrophilicity.

Other minerals such as pyrite and calcite exhibit weak to moderate water-wetting behavior, as they have weaker polar bonds. The effects of different minerals on wettability were investigated for all 29 samples after they were classified into three types, based on their hydrophilicity (strongly, moderately, and weakly water-wet). The mineral content and the corresponding wettability index (I) obtained through the Amott−Harvey method were averaged for each sandstone type, and are shown in Figure 3.

Figure 3 shows that the amounts of different minerals affect sandstone wettability. Although they are all water-wet minerals, pyrite, carbonate, and clay minerals negatively affect sandstone hydrophilicity, while quartz has a positive effect, and this was confirmed by other work.[35−37] Based on our 29 samples, the range and average content of each mineral for these three types of sandstones are listed in Table 3.

3.3.2. Impact of Organic Matter. As shown in Figure 4, the main feature of tight sandstones in coal measures is that they are rich in organic carbon.

It was found that strongly hydrophilic sandstones contain much less organic matter than weakly hydrophilic sandstones.

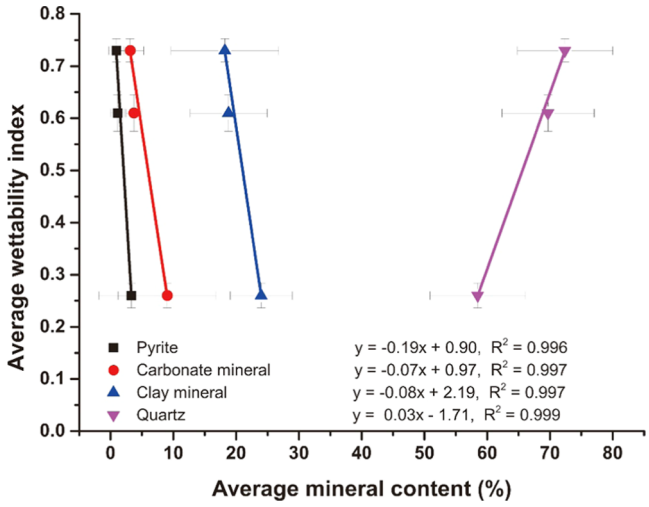

Figure 3. Relationship between the average mineral content and the wettability index for sandstone.

Most strongly hydrophilic sandstones do not contain organic matter (Figure 4a), while a few contain small amounts of coal fragments or the carbonaceous mudstone strip (Figure 4b). The average area ratio of organic matter on the core for these strongly hydrophilic sandstones is 0.2%, while the range is from 0 to 0.7%. These strongly hydrophilic sandstones are usually the middle part of the thick sandstone layer, which are light-gray coarse and medium grain sandstone. The carbonaceous mudstone strip sandwiched in the sandstone reflects the intermittent drop of hydrodynamic force in the strongly hydrodynamic sedimentary environment.

The moderately hydrophilic sandstones contain coal fragments (Figure 4c) and the carbonaceous mudstone strip (Figure 4d), they are mostly gray coarse and medium-grained sandstones, and they are darker than strongly hydrophilic sandstones. The average area ratio of organic matter on the core is 1.4% with a range of 0.5−3.3%.

Weakly hydrophilic sandstones generally have a high amount of organic matter, with an average surface area of 4.5%, so the rock has the darkest color. Among these there are two types of sandstone, one is gray-black fine sandstone with a large amount of the carbonaceous mudstone strip (Figure 4e), where the area of organic matter can reach 5.5−10.0%, and the other one is dark gray medium fine sandstone with more various carbonaceous fragments (Figure 4f), where the organic matter accounts for 1−4.4% of the total area. These weakly hydrophilic sandstones are generally in the top section of sandstone layers, and they are often adjacent to carbonaceous mudstone or coal beds. The large number of thin layers of mudstone sandwiched in the sandstone reflects the overall weak and turbulent hydrodynamics of the sedimentary environment.

It should be noted that organic carbon is similar to coal in the contact angle (around 60−70°), Therefore, the rich organic carbon in the sandstone can reduce its hydrophilicity; especially, when a large amount of finely dispersed organic carbon and fine sand particles is uniformly mixed to form a gray-black sandstone, the contact angle of the sandstone will be significantly increased. This can explain why sample 23 has a much higher contact angle than others.

3.3.3. Impacts of the Sedimentary Environment and Sandstone Texture. Controlled by the sedimentary environment, the mineral composition, texture (including grain size),

https://doi.org/10.1021/acsomega.2c03288
ACS Omega 2022, 7, 28503−28515

Table 3. Average Content of Each Mineral for These Three Types of Sandstones

	sandstones					
	strongly water-wet		moderately water-wet		weakly water-wet	
minerals	range (%)	average (%)	range (%)	average (%)	range (%)	average (%)
quartz	63−87	72.4	55−77	69.7	46−69	58.5
clay minerals	5−25	18.2	10−25	18.8	15−35	24.0
carbonate minerals	1−9	3.1	2−10	3.7	2−30	9.0
pyrite	0−2	0.9	1−2	1.1	1−20	3.3

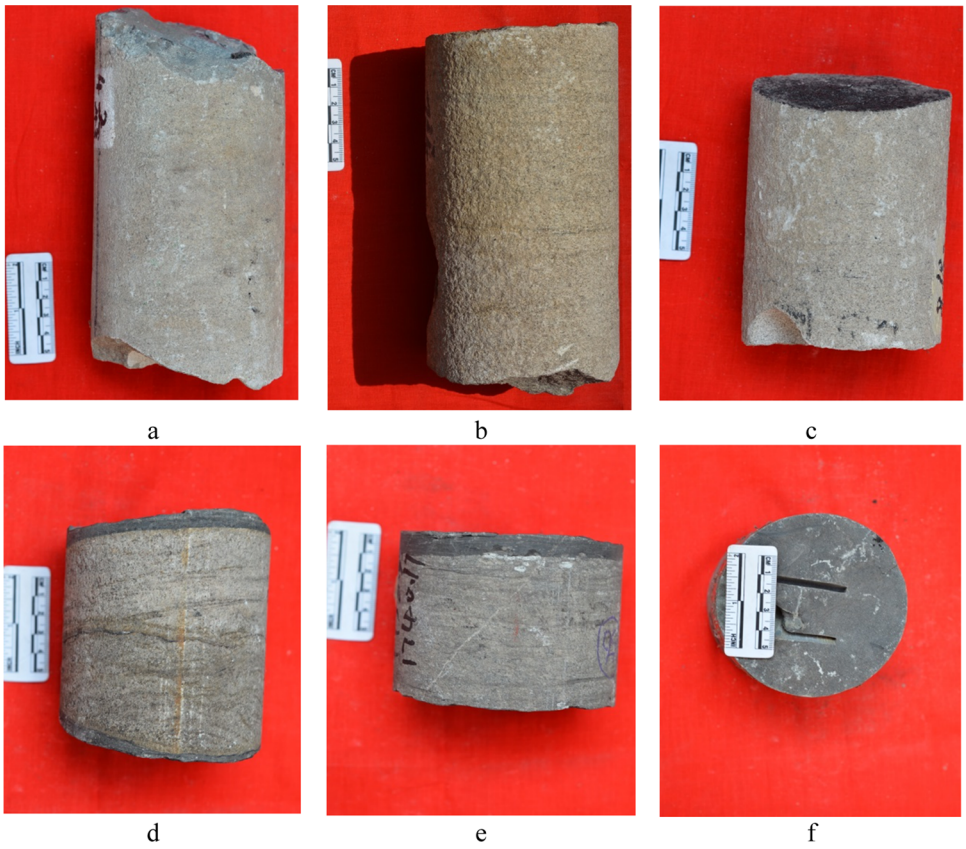

Figure 4. Organic matter in sandstones with different wettabilities: (a) sample 5, strongly hydrophilic, and no organic matter; (b) sample 10, strongly hydrophilic, and a small amount of carbonaceous mudstone strip; (c) sample 1, hydrophilic, and rich in a continuous thin coal fragment layer; (d) sample 12, hydrophilic, and sandwiched with carbonaceous mudstone strip and mudstone; (e) sample 11, weakly hydrophilic, a large amount of carbonaceous mudstone strip, and rich in dispersed organic matter; and (f) sample 23, weakly hydrophilic, a large amount of carbonaceous mudstone strip, and rich in dispersed organic matter.

porosity, permeability, and hydrophilicity of sandstone are a set of indicators with internal correlation. The details are presented as follows:

As shown in Table 4, the sandstone sample has a porosity ranging from 1.20−9.50% and a permeability ranging from 0.002 to 4.324 × 10^{-3} μm^2. These values mean that the sandstones serve as the gas reservoir with very low porosity and permeability. In general, with an increase in the porosity, permeability is also improved, as shown in Figure 5, because better pore development brings better pore−throat connectivity. The porosity and permeability are greatly affected by the sandstone grain size. Figure 6 shows the positive effect of grain size on porosity (Figure 6a) and permeability (Figure 6b). It should be noticed that sample 23 represented an out-of-range point, considering there are a lot of dispersed organic matters and some microfractures in this sample. During sampling or experiment, the weak points in the sandstone tend to expand along the original small cracks, and this change was enhanced by soft organic matter. The development of fractures significantly enhances the sandstone permeability, despite that the porosity of sandstone is low. This phenomenon is rare in the tight sandstones from the study area.

In addition, the strongly water-wet sandstones are found to have a higher porosity (4.01−9.50%, avg.: 6.28%) than those of the moderately water-wet sandstones (3.49−9.40%, avg.: 5.51%) and weakly water-wet ones (1.20−6.50%, avg.: 3.90%). The relationship between the porosity and the wettability index for these 29 of sandstones is shown in Figure 7.

In general, the increase in the porosity will bring a higher wettability index. In the wettability experiment, the large porosity provides a large space for water storage; meanwhile, due to the high permeability and good pore−throat connectivity, the water can be smoothly drawn into the pores. In this way, the sandstone with large porosity and large permeability can absorb water continuously, with a large hydropathic index and high hydrophilicity. This positive correlation between

https://doi.org/10.1021/acsomega.2c03288
ACS Omega 2022, 7, 28503−28515

Table 4. Sandstone Porosity and Permeability Results Obtained through MIP Tests

sample no.	porosity (%)	permeability (10^{-3} μm^2)	sample no.	porosity (%)	permeability (10^{-3} μm^2)
1	4.75	0.028	16	5.13	0.040
2	3.82	0.017	17	2.32	0.003
3	5.90	0.009	18	6.42	0.085
4	5.81	0.008	19	4.01	0.008
5	4.51	0.006	20	9.50	0.055
6	3.50	0.007	21	6.50	0.051
7	6.30	0.033	22	4.80	0.007
8	6.06	0.035	23	2.30	4.324
9	9.40	0.037	24	9.30	0.050
10	4.57	0.030	25	4.88	0.103
11	1.20	0.002	26	8.48	0.183
12	3.49	0.007	27	3.90	0.005
13	5.13	0.040	28	4.75	0.003
14	3.80	0.004	29	1.90	0.004
15	6.31	0.102			

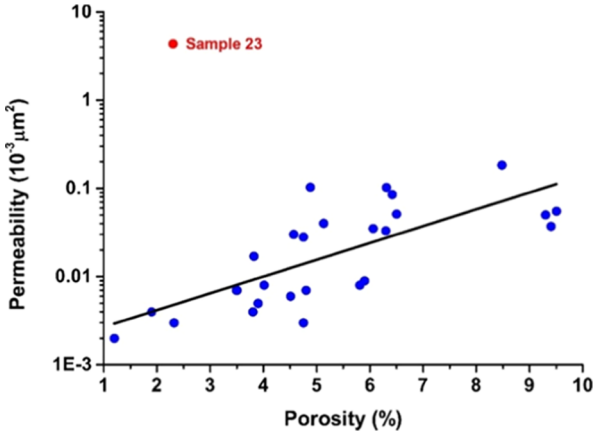

Figure 5. Positive relationship between the sandstone porosity and permeability.

hydrophilicity and porosity and permeability is very favorable for gas reservoir exploitation. As the hydrophilicity, porosity, and permeability of sandstone increase, water enters the sandstone more easily during the water flooding process. Consequently, more gas is displaced, and the gas recovery of the tight gas reservoir is improved. In addition, tight sandstone with high porosity and permeability generally has a higher gas content because it can provide a larger space for reservoir gas. Thus, the gas production of this type of tight sandstone is higher.

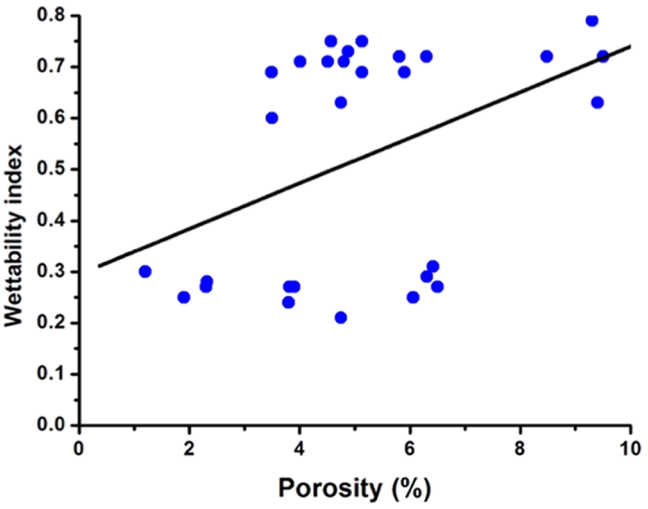

Figure 7. Relationship between the porosity and the wettability index.

It should be noted that the relationship between the porosity, permeability, particle size, and wettability of sandstone can be traced back to the sedimentary period of sandstone. It is discussed as follows:

The sandstone formed in the strongly hydrodynamic sedimentary environment has a coarse particle size, good separation, high quartz content, and fine particles such as clay are washed away by the water flow. Therefore, the sandstone has high porosity, high permeability, and good pore−throat connectivity. This sandstone is often light-colored coarse-medium-grained quartz sandstone or detrital quartz sandstone. In the Amott−Harvey experiment, under the attraction of hydrophilic minerals, water was sucked into the sandstone. Because the pores penetrate well, they can inhale a large volume of water at a fairly fast speed; thus, the sandstone exhibits a large water-wetting index. At the same time, the sandstone has poor oil absorption capacity and low oil-wetting index since the minerals are hydrophilic.

The sandstone formed in the weakly hydrodynamic environment has a fine particle size and a low quartz content. A large

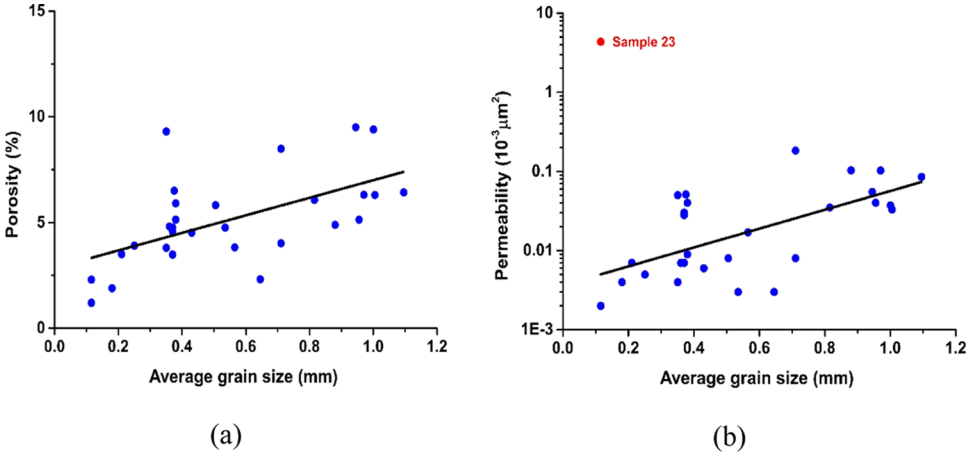

Figure 6. Effects of average sandstone grain size on (a) porosity and (b) permeability.

https://doi.org/10.1021/acsomega.2c03288
ACS Omega 2022, 7, 28503−28515

Table 5. Summary of Characterizations of Sandstones from Figure 8

type	sedimentary environment	hydrodynamic force	physical characteristics	hydrophilicity
1	barrier bar, the main body of the subaqueous distributary channel (excluding the top and bottom part), and the sand flat	strong	coarse particle size, high quartz content, low clay and organic matter content, and high porosity	moderately to strongly hydrophilic
2	mixed flat, river mouth bar, subaqueous natural levee, and interdistributary bays	weak	finer grain size, lower quartz content, higher clay and organic matter content, and lower porosity	weakly hydrophilic

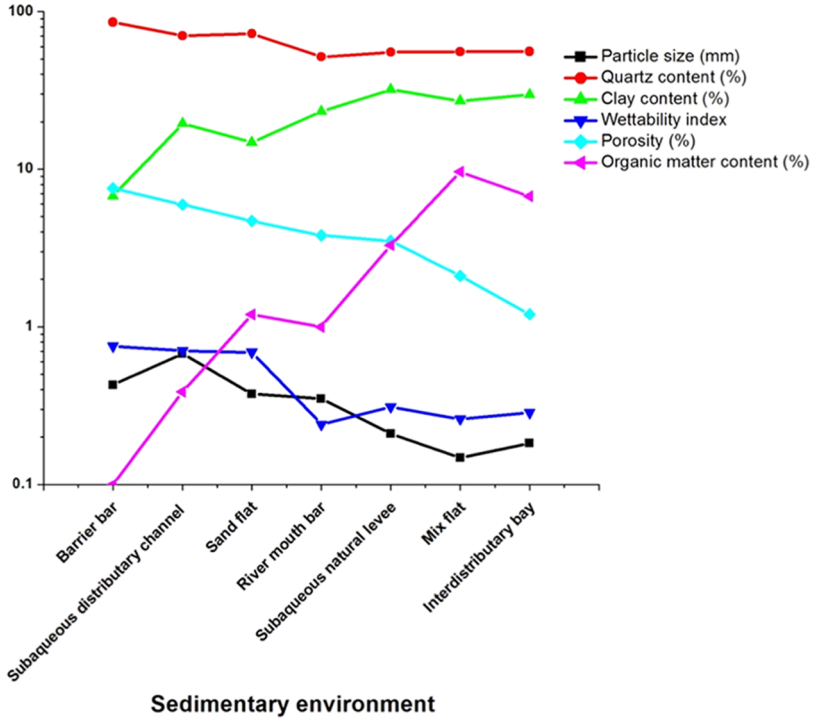

Figure 8. Relationship between the sedimentary environment and sandstone parameters.

amount of heterogeneous clay and organic matters is mixed and deposited, blocking the pores, resulting in low porosity and permeability of the sandstone. It forms gray-black fine-grained debris sandstone with a large amount of carbon-bearing mudstone stripes. In the Amott−Harvey experiment, because the pores were blocked, only a small amount of water was sucked into the sandstone, showing a lower water-wet index; also, because of the high organic matter content, the sandstone enhanced oil absorption capacity, showing a slightly higher oil-wet index; eventually, this sandstone shows a lower wettability index and weak hydrophilicity. Therefore, various sedimentary environments control the composition and structure of the sandstone through hydrodynamic conditions, thus affecting the wettability of the sandstone.

In the study area, the sedimentary environment in the Benxi Formation and Taiyuan Formation is a sea-land transitional facies, and the Shanxi Formation is a shallow water delta environment. The sandstones of the Benxi Formation are formed in sedimentary microfacies such as barrier bars, sand flats, and mixed flats. The sand bodies of Taiyuan and Shanxi Formations are mainly formed in sedimentary microfacies such as shallow delta subaqueous distributary channels, river mouth bars, and subaqueous natural levees. A small amount of thin sandstone can be formed in the interdistributary bay. Based on information such as petrological characteristics, sedimentary structure, and logging, we analyzed the sedimentary microfacies of each sample. Then, the relationship between sedimentary microfacies and sandstone parameters was established, as shown in the figure below.

Table 5 describes summarized conclusions of the findings from Figure 8.

It should be noted that sandstone hydrophilicity weakens in sequence in the following sedimentary environment: barrier bars, main bodies of subaqueous distributary channels, sand flats, subaqueous natural levees, river mouth bars, mixed flats, and interdistributary bays. The influencing factors of sandstone wettability mainly rely on the material basis of sandstone such as the composition and structure rather than the depositional environment. Therefore, the influencing factors of wettability in different depositional environments may be comparable.

3.3.4. Impact of Diagenesis and Mineral Occurrence. Under a microscope, a sandstone generally consists of three components: particles, interstitial materials, and pores. The thin-section analysis of the sandstone lithology is shown in Figure 9.

Figure 9 illustrates that the sandstones in the study area were mainly litharenite (58.6%), with some lithic quartz arenite (24.1%), feldspathic litharenite (13.8%), and a small amount of quartz arenite (3.4%). Figure 10 shows the mineral occurrence and texture of sandstones through microscopy and SEM analysis.

As shown in Figure 10a, the clastic particles are mainly quartz, along with lithic fragments that were composed of low-grade metamorphic carbonaceous argillaceous slate and sericite phyllite. The interstitial materials between the particles are

https://doi.org/10.1021/acsomega.2c03288
ACS Omega 2022, 7, 28503−28515

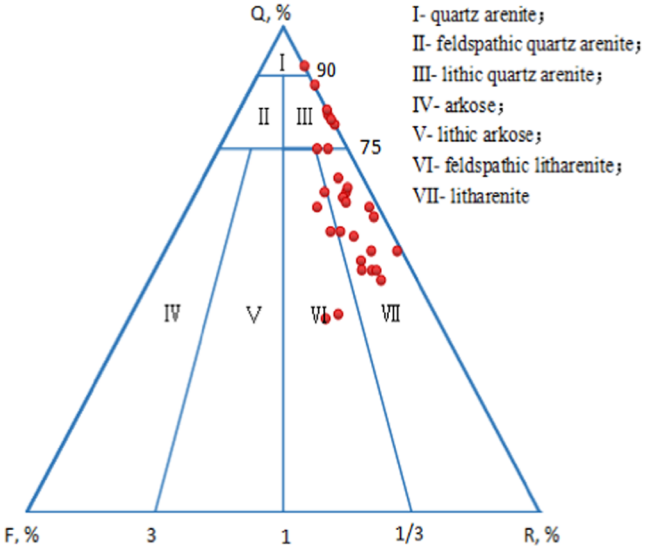

Figure 9. Ternary plot showing the sandstone lithology where Q, F, and R represent quartz, feldspar, and rock fragment, separately.

mud matrix, followed by ankerite (Figure 10a,b); quartz overgrowths (Figure 10c); carbonate minerals (calcite, siderite), pyrite, and book-like authigenic kaolinite (Figure 10e); and authigenic quartz crystal and filamentous authigenic illite (Figure 10f). The particles are subangular to subrounded, moderately to well sorted with porous cementation. Figure 10c,d also reveals that the pores in sandstone are dominated by interparticle, intraparticle, and moldic dissolution pores, with a diameter ranging from 0.01−0.60 mm. Some subordinate residual primary intergranular and intercrystalline pores (Figure 10e,f) can also be seen. The pore throats generally have sheet-like, bending-flake-like or tubular geometry.

Based on Figure 10, we can explain why minerals behave differently with regard to sandstone wettability although they are all water-wet. The occurrence of minerals has a certain influence on the wettability of sandstone. Generally, quartz exists as the main rigid skeleton particles; a higher quartz content will result in more pore spaces for water to be absorbed into sandstone. An increase in the quartz content will enhance the sandstone water-wetting behavior. Meanwhile, pyrite, clay, and carbonate minerals exist as interstitial materials, blocking pore spaces and thus, preventing water from infiltrating the sandstone. An increase in the value will deteriorate the sandstone water-wetting behavior.

It should be noted that under a microscope, most sandstones in the study area are as shown in Figure 10a,b; it can be seen that the pores are generally not developed, and they are generally poorly connected and are occluded by detrital or authigenic clay minerals or strong carbonate cement.

This kind of strong compaction generally exists in tight sandstones of coal series, and it has a great influence on the wettability of sandstones. There are a lot of argillaceous slate and mud matrix mixed with dispersed organic matter in the sandstone (Figure 10a). Clay and organic matter are both

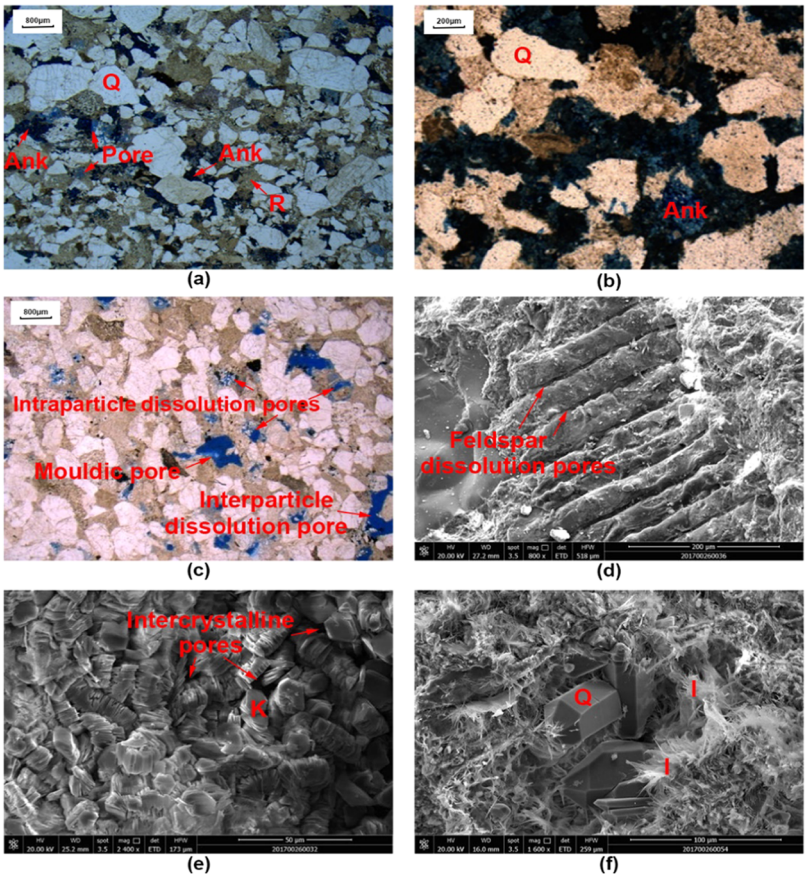

Figure 10. Mineral occurrences and textures of sandstone through microscopy and SEM analysis: (a) sample 7, plane-polarized light, 12.5X, Q: quartz, R: rock fragment, and Ank: ankerite; (b) sample 17, plane-polarized light, and 50X; (c) sample 20, plane-polarized light, and 12.5X; (d) sample 6, SEM image, and 800X; (e); sample 10, SEM image, 2400X, and K: kaolinite; and (f) sample 21, SEM image, 1600X, and I: illite.

https://doi.org/10.1021/acsomega.2c03288
ACS Omega 2022, 7, 28503−28515

Table 6. Amott−Harvey Test Results Performed under Different Water Bath Temperatures

	main mineral composition					wettability index (I)		
sample no.	quartz	feldspar	siderite	ankerite	clay minerals	30 °C	40 °C	60 °C
3	67.7	7.0		4.6	17.0	0.69	0.72	0.73
6	55.3	6.5	1.1	1.3	32.0	0.60	0.67	0.70
9	69.2	2.0	3.1		22.6	0.63	0.69	0.71
14	51.6	8.2	13.2	2.0	23.2	0.24	0.28	0.32
20	64.3	1.8	1.1		29.8	0.72	0.74	0.75
24	87.1	1.8			4.8	0.79	0.80	0.81

fine-grained and lighter minerals, which are easily mixed together and deposited when the hydrodynamic force is weakened. This weak argillaceous slate and mud matrix form a highly deformable organic clay under strong compaction, filling the entire pores, greatly reducing the porosity in the sandstone, and the overall hydrophilicity of the sandstone becomes poor. It is because clay minerals are associated with organic matter and have the function of blocking pores, so the higher the clay content in the sandstone, the weaker the sandstone hydrophilicity. This also explains why clay is a strong hydrophilic mineral, but the clay mineral content in sandstone is inversely proportional to the hydrophilicity.

Various ions in the mudstone are transported into the sandstone by underground water and deposited to form carbonate cement. The bottom of the subaqueous distributary channel facies caused a large amount of mudstone debris in the sandstone due to erosion, and the top of the subaqueous distributary channel facies brought a large proportion of muddy texture in the sandstone due to the decrease in the hydrodynamic force. This caused a large number of pores to disappear (Figure 10b). Although this part of the sandstone may still have a coarser particle size, it is weakly hydrophilic due to the disappearance of pores. In the thin sandstone (fine grain) or the top (medium grain, fine grain) and bottom (coarse grain) of the thick sandstone, because of strong carbonate cementation, the sandstone is often weakly hydrophilic.

3.4. Impacts of Sandstone Fluid Properties on Wettability. Unlike the structural forces discussed in the previous section, the sandstone fluids mainly affect the sandstone wettability through the dispersion force and electrostatic force. Generally, the dispersion force is a result of the van der Waals interaction between the molecules of the liquid and the solid surface, and the electrostatic force results from the osmotic pressure caused by the excess counterions present in the liquid interlayer to satisfy the electroneutrality condition.[38] Thus, the effects of fluid temperature and other properties, including brine type, salinity, and pH, on sandstone wettability are explored.

3.4.1. Impacts of Temperature. Six representative samples were selected out of these 29 sandstone samples to test the effect of temperature change on wettability. Amott−Harvey tests were performed under three different water bath (30 g/L $CaCl_2$ solution) temperatures. The results are listed in Table 6.

The relationship between temperature and wettability for these six sandstone samples is also illustrated in Figure 11.

As shown in Figure 11, with an increase in water bath temperature, the wettability index of the sandstone increases, and the increase is almost linear. There is also an inconspicuous trend: the higher the temperature, the lower the increase in hydrophilicity. It was also noticed that below 60 °C, sample 14 changes from weakly water-wet to moderately water-wet.

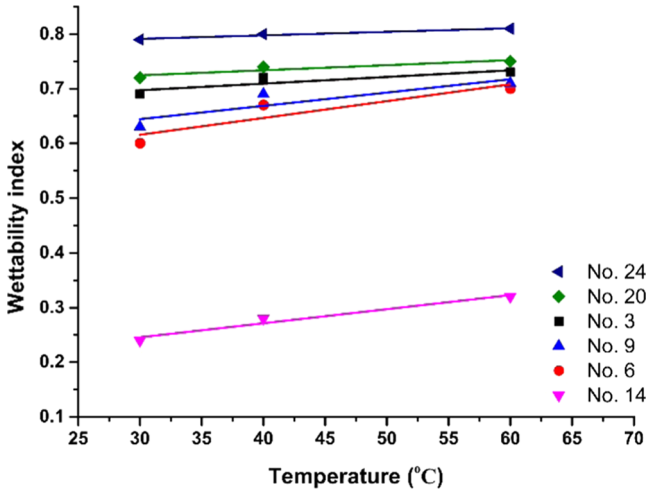

Figure 11. Relationship between temperature and wettability.

This phenomenon can be explained as follows: in the rock−brine system, the interfacial tension at the solid−liquid interface is a result of van der Waals interactions. With an increase in temperature, the liquid surface tension is reduced at a much higher rate than the solid surface tension, as the increased thermal vibrations of water droplets weaken the van der Waals interaction.[38,39] This was confirmed by our results, showing that an increase in temperature from 30 to 60 °C results in a decrease in the surface tension of a 30 g/L $CaCl_2$ solution from 69.37 to 60.25 mN/m. Meanwhile, the solid−liquid interfacial tension also decreases, causing better affinity of solid to liquid; thus, the hydrophilicity increases. It should also be noted that with an increase in temperature, the hydrophilicity of sandstone containing higher amounts of clay minerals also increases at a higher rate. This is because the van der Waals interaction between water and clay minerals is stronger than that between water and quartz.[40]

3.4.2. Impacts of Fluid Type, Salinity, and pH. Amott−Harvey tests and contact angle measurements were performed on several samples by changing the fluid type, salinity, and pH while keeping all other parameters constant. These factors mainly affect sandstone wettability through electrostatic interactions.

3.4.2.1. Impacts of Fluid Type and Salinity. The contact angles between sandstone and water, NaCl, $NaHCO_3$, $CaCl_2$, and $MgCl_2$ solutions were measured. The concentrations of the solutions were all 30 g/L. The results are shown in Figure 12.

It can be seen that for all 10 samples, compared with water, all salt solutions result in a larger contact angle and lower hydrophilicity; at the same mass concentration, calcium and magnesium ions increase the contact angle and decrease the hydrophilicity, compared with sodium ions. To further explore the cause of different wetting behaviors, the impacts of different

https://doi.org/10.1021/acsomega.2c03288
ACS Omega 2022, 7, 28503−28515

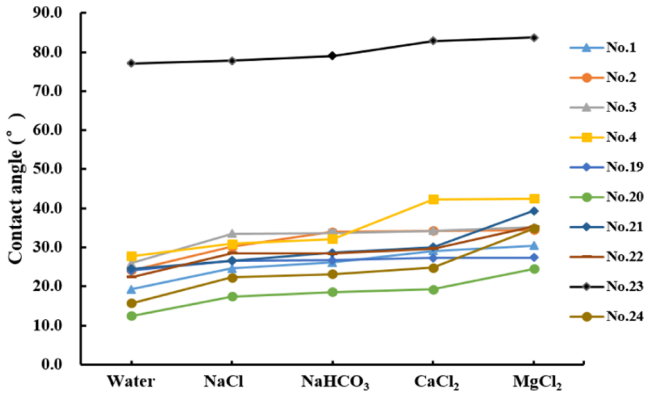

Figure 12. Relationship between fluid type and wettability.

concentrations of $CaCl_2$ on sandstone wettability are shown in Figure 13.

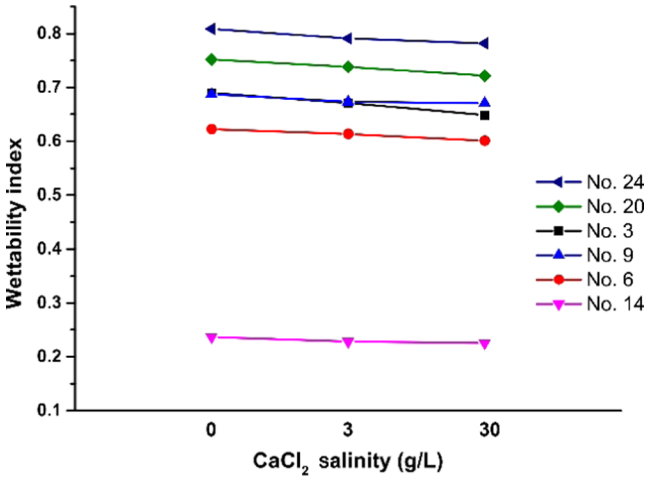

Figure 13. Impacts of $CaCl_2$ salinity on wettability.

It can be seen that with an increase in salinity, the hydrophilicity decreases. The phenomena that were observed in Figures 12 and 13 can be explained as follows: the water film absorbed on the rock surface was strongly influenced by the electrostatic potential at the solid−liquid interface. The ionic strengths of NaCl, $NaHCO_3$, $CaCl_2$, and $MgCl_2$ solutions increase, in turn, under the same concentration, while the ionic strengths of 0, 3, and 30 g/L $CaCl_2$ solutions increase, in turn. Increasing the ionic strength in the solution (that is, increasing the ion concentration and valence) makes the thickness of the electric double layer thinner, that is, a more concentrated solution of counterions realizes the charge balance between the electric double layer and the electrostatic charge on the mineral surface in a shorter distance. This leads to thinning of the water film, which results in lower hydrophilicity of the solid surface.[40]

3.4.2.2. Impacts of pH. To investigate the effects of pH on sandstone wettability, Amott−Harvey tests were performed using a 3 g/L $CaCl_2$ solution at three different pH values (5, 7, 8.5). The results are shown in Figure 14.

Figure 14 shows that, in general, an increase in pH corresponds to a relatively small increase in sandstone wettability. This agrees with many other works.[41−43] It is believed that a change in pH brings a change in electric charge. Thus, ζ-potential tests were performed to further explore the change in the electrostatic repulsion between the sandstone

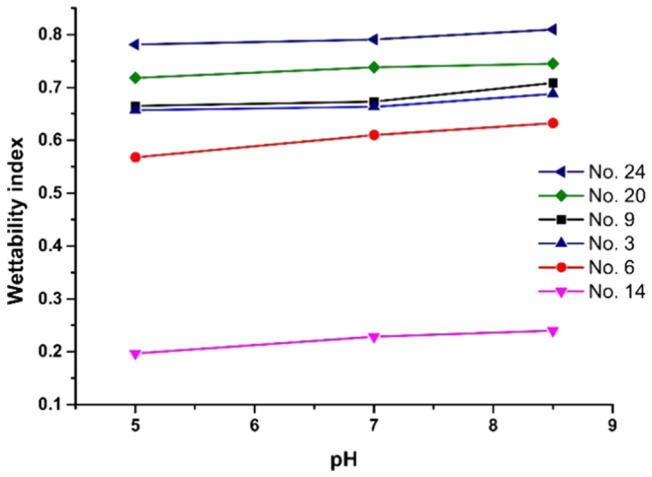

Figure 14. Impacts of fluid pH on sandstone wettability.

particle double layers under different pH values. Here, samples 14, 20, and 24, as well as pure quartz, were tested. Quartz was selected because it is the major component of sandstone. The tests were performed at pH values from 3 to 10. The result is shown in Figure 15.

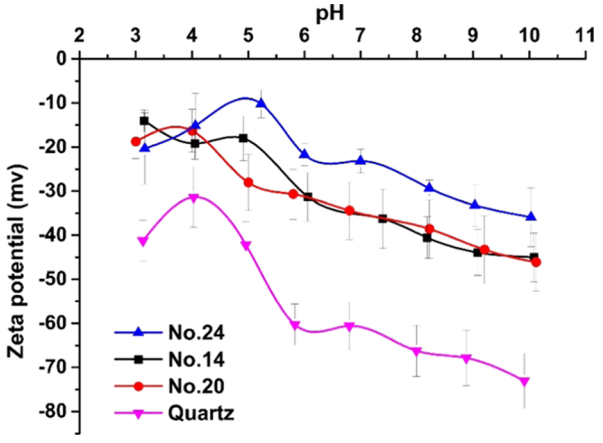

Figure 15. ζ-Potential curve as a function of pH.

As can be seen from Figure 15, under the test condition, the ζ-potential is always negative; this is because the quartz tested always has negative charges on its surface. Furthermore, generally, an increase in pH corresponds to an increase in the ζ-potential, which means that the electric charge increases. Thus, the thickness of the water film that the solid surface can support by the larger-magnitude electrostatic potentials also increases.[44,45] The greater the thickness of the water film, the stronger the hydrophilicity.[38] This further supports the results found in Figure 14. Therefore, an alkaline liquid should be used in the process of water flooding to improve gas recovery.

4. CONCLUSIONS

Three conclusions can be presented from this study and they are listed as follows.

(1) Tight sandstones in coal measures are water-wet with the following physical characteristics. In general, it has low porosity and permeability with small and poor-connected pores and throats. The reservoir rocks are mainly litharenite and lithic quartz arenites with low composi-

https://doi.org/10.1021/acsomega.2c03288
ACS Omega 2022, 7, 28503−28515

tional maturities and moderate textural maturities. The strongly water-wet coarse-grained quartz arenite and lithic quartz arenite, often with high porosity, permeability, and gas content, are the preferred target for the exploration of a tight sandstone gas field.

(2) Microscopically, the sandstone wettability is directly controlled by the combination of three surface forces, including structural force, electrostatic force, and dispersion force, between solid and liquid. It is found that the sandstone surface structure and compositions mainly affect the structural force. The dispersion force is mainly affected by the temperature, and the solution salinity and pH contribute most to the electrostatic force. More quartz, higher surface toughness, higher temperature, as well as lower fluid salinity and higher pH, result in improved water-wetting behavior for sandstones.

(3) The sedimentary environment and diagenesis control the wettability of sandstone by controlling the mineral composition, organic matter content, and structure of sandstone. The sandstone deposited in the strong hydrodynamic barrier bar, the main body of the subaqueous distributary channel (excluding the top and bottom part), and the sand flat are mostly moderately to strongly hydrophilic. Sandstones deposited in weak hydrodynamic forces such as the river mouth bar, subaqueous natural levees, mixed flats, and interdistributary bays are generally weakly hydrophilic. The strong organic clay compaction and carbonate cementation greatly reduce the hydrophilicity of sandstone.

AUTHOR INFORMATION

Corresponding Author

Hao Ma − *BGRIMM Technology Group, Beijing 100070, China;* orcid.org/0000-0001-7253-734X; Email: haoma@bgrimm.com

Authors

Xuejuan Song − *School of Civil Engineering, Xuzhou University of Technology, Xuzhou 221018 Jiangsu, China;* orcid.org/0000-0003-3372-5430

Yong Qin − *School of Resources and Geoscience, China University of Mining and Technology, Xuzhou 221116 Jiangsu, China;* orcid.org/0000-0002-7478-8828

Complete contact information is available at: https://pubs.acs.org/10.1021/acsomega.2c03288

Notes

The authors declare no competing financial interest.

ACKNOWLEDGMENTS

This work was supported by the National Natural Science Foundation of China (No. 42002193) and the Ministry of Science and Technology of China through the Foreign Youth Talent Program (QN2021074001L).

REFERENCES

(1) Afrapoli, M. S.; Crescente, C.; Alipour, S.; Torsaeter, O. The effect of bacterial solution on the wettability index and residual oil saturation in sandstone. *J. Pet. Sci. Eng.* **2009**, *69*, 255−260.

(2) Morrow, N. R. Wettability and its effect on oil recovery. *J. Pet. Technol.* **1990**, *42*, 1476−1484.

(3) Bordeaux-Rego, F.; Mehrabi, M.; Sanaei, A.; Sepehrnoori, K. Improvements on modelling wettability alteration by Engineered water injection: Surface complexation at the oil/brine/rock contact. *Fuel* **2021**, *284*, No. 118991.

(4) Bonn, D.; Eggers, J.; Indekeu, J.; Meunier, J.; Rolley, E. Wetting and spreading. *Rev. Mod. Phys.* **2009**, *81*, 739−805.

(5) Drummond, C.; Israelachvili, J. Surface forces and wettability. *J. Pet. Sci. Eng.* **2002**, *33*, 123−133.

(6) Cuiec, L. E. Restoration of the Natural State of Core Samples. In *Fall Meeting of the Society of Petroleum Engineers of AIME*; Society of Petroleum Engineers: Dallas, Texas, 1975.

(7) Basu, S.; Sharma, M. M. Investigating the Role of Crude-Oil Components on Wettability Alteration using Atomic Force Microscopy. In *International Symposium on Oilfield Chemistry*; Society of Petroleum Engineers: Houston, Texas, 1997.

(8) Buckley, J. S.; Liu, Y.; Monsterleet, S. Mechanisms of wetting alteration by crude oils. *SPE J.* **1998**, *3*, 54−61.

(9) Kaminsky, R.; Radke, C. J. *Water Films, Asphaltenes, and Wettability Alteration (No. DOE/FEW-4680)*; Lawrence Berkeley Lab.: CA (United States), 1998.

(10) Chandrasekhar, S.; Sharma, H.; Mohanty, K. K. Dependence of wettability on brine composition in high temperature carbonate rocks. *Fuel* **2018**, *225*, 573−587.

(11) Liang, T.; Zhou, F.; Lu, J.; DiCarlo, D.; Nguyen, Q. Evaluation of wettability alteration and IFT reduction on mitigating water blocking for low-permeability oil-wet rocks after hydraulic fracturing. *Fuel* **2017**, *209*, 650−660.

(12) Hirasakl, G. J. Wettability: fundamentals and surface forces. *SPE Form. Eval.* **1991**, *6*, 217−226.

(13) Lamb, R. N.; Furlong, D. N. Controlled wettability of quartz surfaces. *J. Chem. Soc., Faraday Trans. 1* **1982**, *78*, 61−73.

(14) Mohammed, I.; Al Shehri, D.; Mahmoud, M.; Kamal, M. S.; Alade, O. S. A surface charge approach to investigating the Influence of oil contacting clay minerals on wettability alteration. *ACS Omega* **2021**, *6*, 12841−12852.

(15) Buckley, J. S.; Lord, D. L. Wettability and morphology of mica surfaces after exposure to crude oil. *J. Pet. Sci. Eng.* **2003**, *39*, 261−273.

(16) Mohammed, I.; Al Shehri, D.; Mahmoud, M.; Kamal, M. S.; Alade, O. S. Impact of Iron Minerals in Promoting Wettability Alterations in Reservoir Formations. *ACS Omega* **2021**, *6*, 4022−4033.

(17) Zhao, Z.; Tao, L.; Guo, J.; Zhao, Y.; Chen, C. A novel wettability index and mineral content curve based shut-in time optimization approach for multi-fractured horizontal wells in shale gas reservoirs. *J. Pet. Sci. Eng.* **2022**, *211*, No. 110192.

(18) Khurshid, I.; Al-Shalabi, E. W. New insights into modeling disjoining pressure and wettability alteration by engineered water: Surface complexation based rock composition study. *J. Pet. Sci. Eng.* **2022**, *208*, No. 109584.

(19) Zou, C.; Zhu, R.; Liu, K.; Su, L.; Bai, B.; Zhang, X.; Yuan, X.; Wang, J. Tight gas sandstone reservoirs in China: characteristics and recognition criteria. *J. Pet. Sci. Eng.* **2012**, *88*−*89*, 82−91.

(20) Yang, T.; Zhang, G.; Liang, K.; Zheng, M.; Guo, B. The exploration of global tight sandstone gas and forecast of the development tendency in China. *Eng. Sci.* **2012**, *14*, 64−68.

(21) Wang, Z.; Luo, X.; Liu, K.; Lei, Y.; Zhang, L.; Cheng, M.; Wang, X. Evaluation of pore-scale wettability in the tight sandstone reservoirs of the Upper Triassic Yanchang Formation, Ordos Basin, China. *Mar. Pet. Geol.* **2022**, *138*, No. 105528.

(22) Jiang, Z.; Liu, Z.; Zhao, P.; Chen, Z.; Mao, Z. Evaluation of tight waterflooding reservoirs with complex wettability by NMR data: A case study from Chang 6 and 8 members, Ordos Basin, NW China. *J. Pet. Sci. Eng.* **2022**, *213*, No. 110436.

(23) Ma, S. M.; Zhang, X.; Morrow, N. R.; Zhou, X. Characterization of wettability from spontaneous imbibition measurements. *J. Can. Pet. Technol.* **1999**, *38*, 1−8.

(24) He, J.; Zhang, X.; Ma, L.; Wu, H.; Ashraf, M. A. Geological characteristics of unconventional gas in Coal Measure of upper Paleozoic coal measures in Ordos Basin, China. *Earth Sci. Res. J.* **2016**, *20*, 1−5.

(25) Cao, D.; Yao, Z.; Li, J. Evaluation status and development trend of unconventional gas in coal measure. *Coal Sci. Technol.* **2014**, *42*, 89−92.
(26) Nakae, H.; Inui, R.; Hirata, Y.; Saito, H. Effects of surface roughness on wettability. *Acta Mater.* **1998**, *46*, 2313−2318.
(27) Kubiak, K. J.; Wilson, M. C. T.; Mathia, T. G.; Carval, P. Wettability versus roughness of engineering surfaces. *Wear* **2011**, *271*, 523−528.
(28) Churaev, N. V. Surface forces in wetting films. *Colloid J.* **2003**, *65*, 263−274.
(29) Govind Rajan, A.; Sresht, V.; Pádua, A. A.; Strano, M. S.; Blankschtein, D. Dominance of dispersion interactions and entropy over electrostatics in determining the wettability and friction of two-dimensional MoS_2 surfaces. *ACS Nano* **2016**, *10*, 9145−9155.
(30) Pashley, R. M.; Israelachvili, J. N. Molecular layering of water in thin films between mica surfaces and its relation to hydration forces. *J. Colloid Interface Sci.* **1984**, *101*, 511−523.
(31) Israelachvili, J. N.; Pashley, R. M. Molecular layering of water at surfaces and origin of repulsive hydration forces. *Nature* **1983**, *306*, 249−250.
(32) Pashley, R. M. DLVO and hydration forces between mica surfaces in Li^+, Na^+, K^+, and Cs^+ electrolyte solutions: A correlation of double-layer and hydration forces with surface cation exchange properties. *J. Colloid Interface Sci.* **1981**, *83*, 531−546.
(33) Papirer, E. *Adsorption on Silica Surfaces*; Marcel Dekker, Inc.: New York, 2000; pp 217−220.
(34) Liu, C. M.; Feng, A. S.; Guo, Z. X.; Cao, X. F.; Hu, Y. H. Dynamics simulation of tertiary amines adsorbing on kaolinite (001) plane. *Trans. Nonferrous Met. Soc. China* **2011**, *21*, 1874−1879.
(35) Alnili, F.; Al-Yaseri, A.; Roshan, H.; Rahman, T.; Verall, M.; Lebedev, M.; Sarmadivaleh, M.; Iglauer, S.; Barifcani, A. Carbon dioxide/brine wettability of porous sandstone versus solid quartz: An experimental and theoretical investigation. *J. Colloid Interface Sci.* **2018**, *524*, 188−194.
(36) Lu, Y.; Tian, R.; Liu, W.; Tang, J.; Li, H.; Chen, X.; Sun, X. Mechanisms of shale water wettability alteration with chemical groups after CO_2 injection: Implication for shale gas recovery and CO_2 geo-storage. *J. Nat. Gas Sci. Eng.* **2021**, *90*, No. 103922.
(37) Lu, Y.; Tian, R.; Tang, J.; Jia, Y.; Lu, Z.; Sun, X. Investigating the mineralogical and chemical effects of CO_2 injection on shale wettability at different reservoir temperatures and pressures. *Energy Fuels* **2021**, *35*, 14838−14851.
(38) Gribanova, E. V. Dynamic contact angles: Temperature dependence and the influence of the state of the adsorption film. *Adv. Colloid Interface Sci.* **1992**, *39*, 235−255.
(39) Van Oss, C. J. *Interfacial Forces in Aqueous Media*; CRC Press: Boca Raton, 2006; pp 1−30.
(40) Tokunaga, T. K. DLVO-based estimates of adsorbed water film thicknesses in geologic CO_2 reservoirs. *Langmuir* **2012**, *28*, 8001−8009.
(41) Churaev, N. V. Wetting films and wetting. *Rev. Phys. Appl.* **1988**, *23*, 975−987.
(42) Kim, Y.; Wan, J.; Kneafsey, T. J.; Tokunaga, T. K. Dewetting of silica surfaces upon reactions with supercritical CO_2 and brine: pore-scale studies in micromodels. *Environ. Sci. Technol.* **2012**, *46*, 4228−4235.
(43) Liu, Y.; Mutailipu, M.; Jiang, L.; Zhao, J.; Song, Y.; Chen, L. Interfacial tension and contact angle measurements for the evaluation of CO_2-brine two-phase flow characteristics in porous media. *Environ. Prog. Sustainable Energy* **2015**, *34*, 1756−1762.
(44) Gribanova, E. V.; Molchanova, L. I.; Grigorov, O. N.; Popova, V. N. pH-dependence of contact angles on glass and quartz. *Colloid J.* **1976**, *38*, 504−506.
(45) Jung, J. W.; Wan, J. Supercritical CO_2 and ionic strength effects on wettability of silica surfaces: Equilibrium contact angle measurements. *Energy Fuels* **2012**, *26*, 6053−6059.

https://doi.org/10.1021/acsomega.2c03288
ACS Omega 2022, 7, 28503−28515